Validation Efforts of an Open-Source Aeroacoustics Model for Wind Turbines

Preprint

Pietro Bortolotti,[1] Yi Guo,[1] Eric Simley,[1] Jason Roadman,[1] Nicholas Hamilton,[1] Patrick J. Moriarty,[1] Carlo R. Sucameli,[2] and Franck Bertagnolio[3]

1 National Renewable Energy Laboratory
2 Technical University of Munich
3 DTU Wind Energy

Presented at the Ninth International Conference on Wind Turbine Noise
May 18–21, 2021

NREL is a national laboratory of the U.S. Department of Energy
Office of Energy Efficiency & Renewable Energy
Operated by the Alliance for Sustainable Energy, LLC

Conference Paper
NREL/CP-5000-79383
July 2021

This report is available at no cost from the National Renewable Energy Laboratory (NREL) at www.nrel.gov/publications.

Contract No. DE-AC36-08GO28308

Validation Efforts of an Open-Source Aeroacoustics Model for Wind Turbines

Preprint

Pietro Bortolotti,[1] Yi Guo,[1] Eric Simley,[1] Jason Roadman,[1] Nicholas Hamilton,[1] Patrick J. Moriarty,[1] Carlo R. Sucameli,[2] and Franck Bertagnolio[3]

1 National Renewable Energy Laboratory
2 Technical University of Munich
3 DTU Wind Energy

Suggested Citation
Bortolotti, Pietro, Yi Guo, Eric Simley, Jason Roadman, Nicholas Hamilton, Patrick J. Moriarty, Carlo R. Sucameli, and Franck Bertagnolio. 2021. *Validation Efforts of an Open-Source Aeroacoustics Model for Wind Turbines: Preprint*. Golden, CO: National Renewable Energy Laboratory. NREL/CP-5000-79383. https://www.nrel.gov/docs/fy21osti/79383.pdf.

NREL is a national laboratory of the U.S. Department of Energy
Office of Energy Efficiency & Renewable Energy
Operated by the Alliance for Sustainable Energy, LLC

This report is available at no cost from the National Renewable Energy Laboratory (NREL) at www.nrel.gov/publications.

Contract No. DE-AC36-08GO28308

Conference Paper
NREL/CP-5000-79383
July 2021

National Renewable Energy Laboratory
15013 Denver West Parkway
Golden, CO 80401
303-275-3000 • www.nrel.gov

NOTICE

This work was authored in part by the National Renewable Energy Laboratory, operated by Alliance for Sustainable Energy, LLC, for the U.S. Department of Energy (DOE) under Contract No. DE-AC36-08GO28308. Funding provided by the U.S. Department of Energy Office of Energy Efficiency and Renewable Energy Wind Energy Technologies Office. The views expressed herein do not necessarily represent the views of the DOE or the U.S. Government. The U.S. Government retains and the publisher, by accepting the article for publication, acknowledges that the U.S. Government retains a nonexclusive, paid-up, irrevocable, worldwide license to publish or reproduce the published form of this work, or allow others to do so, for U.S. Government purposes.

This report is available at no cost from the National Renewable Energy Laboratory (NREL) at www.nrel.gov/publications.

U.S. Department of Energy (DOE) reports produced after 1991 and a growing number of pre-1991 documents are available free via www.OSTI.gov.

Cover Photos by Dennis Schroeder: (clockwise, left to right) NREL 51934, NREL 45897, NREL 42160, NREL 45891, NREL 48097, NREL 46526.

NREL prints on paper that contains recycled content.

Validation Efforts of an Open-Source Aeroacoustics Model for Wind Turbines

Pietro Bortolotti, National Renewable Energy Laboratory, USA: pietro.bortolotti@nrel.gov
Yi Guo, National Renewable Energy Laboratory, USA
Eric Simley, National Renewable Energy Laboratory, USA
Jason Roadman, National Renewable Energy Laboratory, USA
Nicholas Hamilton, National Renewable Energy Laboratory, USA
Patrick J. Moriarty, National Renewable Energy Laboratory, USA
Carlo R. Sucameli, Technical University of Munich, Germany
Franck Bertagnolio, DTU Wind Energy, Denmark

Summary

The open source aeroservoelastic wind turbine solver, OpenFAST, now includes an aeroacoustics model, which is described here and validated against experimental measurements recorded on a GE 1.5-MW wind turbine installed at the Flatirons Campus of the National Renewable Energy Laboratory in Boulder, Colorado. The validation demonstrates satisfactory agreement between numerical predictions and experimental recordings, with discrepancies up to 7 dB in the overall sound pressure levels at low wind speeds and a better agreement around the rated wind speed of the turbine.

1. Introduction

A higher penetration of wind into the energy mix implies a higher number of wind turbines installed both offshore and on land. Land-based wind farms are often already located in close proximity to residential areas, and the installation of larger turbines in areas subjected to noise generation limits is expected to continue. To estimate compliance with such limits, numerical models that estimate the aeroacoustics emissions of wind turbines are crucial to assist turbine manufacturers in designing quieter turbines and operators with noise-mitigation strategies while minimizing energy production and revenue losses. The National Renewable Energy Laboratory (NREL) has years of experience in developing numerical models to estimate airfoil noise (Moriarty, 2005) and wind turbine noise (Moriarty and Migliore, 2003, Moriarty et al., 2005). While the confidence in the airfoil models has been satisfactory, thanks to decades-old validation campaigns (Amiet, 1975, Brooks et al., 1989), the models to estimate the aeroacoustics noise of wind turbines have been less reliable and have had less documented validation.
Recently, researchers moved the NREL wind turbine aeroacoustics code into the latest release of the open source aeroservoelastic framework, OpenFAST (Bortolotti et al., 2020). While reimplementing the models, a code-to-code comparison against a similar code at the Technical University of Munich was executed (Sucameli et al., 2018). The comparison highlighted some discrepancies, opened new questions, and did not provide any indication about the accuracy of the models in predicting the noise of modern turbines. In this work, those discrepancies are investigated, and a validation effort based on experimental measurements obtained from a GE 1.5-MW wind turbine installed at NREL is presented.

The paper is organized as follows: Section 2 introduces the framework used to run the numerical simulations. The experimental setup and the recorded measurements are presented in Section 3; followed by the results of the validation process, which are discussed in Section 4. Section 5 closes the paper with key takeaways and an overview of the ongoing work.

2. Numerical Models and Code-to-Code Verifications

OpenFAST includes a variety of models to estimate the aeroacoustics noise of wind turbines (Bortolotti et al., 2020). The next two subsections elaborate on the two models that were verified and validated in past work. The first model aims to capture the noise generated along the leading edges (LEs) of the blades, the second model along the trailing edges (TEs). All other noise sources are excluded from the analysis and are assumed to make minor contributions to the total noise levels.

2.1 Leading-edge noise

The turbulent inflow noise represents the noise generated by an arbitrary body immersed in a turbulent flow. For a wind turbine, we assume that this noise radiates from the LE of the rotor blades. To predict turbulent inflow (TI) noise, OpenFAST implements the Amiet model (Amiet, 1975), which adopts a flat-plate approximation. A correction for finite blade thicknesses has also been developed and implemented (Moriarty et al., 2005), and is added to the Amiet sound pressure levels (SPLs). In this work we restricted the verification and validation processes to the Amiet model, which computes the SPL of an airfoil as

$$SPL_{TI} = 10\log_{10}\left(\rho^2 c^4 \frac{L_t d}{2r_e^2} M^5 I_1^2 \frac{\hat{k}_1^3}{\left(1+\hat{k}_1^2\right)^{\frac{7}{3}}} \overline{D}\right) + 78.4 \quad (1)$$

where ρ is the air density, c the speed of sound, L_t the turbulent length scale, d the blade element span, r_e the effective distance between LE and observer, M the Mach number, I_1 the turbulence intensity of the airfoil inflow, $\hat{k}_1$ a wave number function of frequency f, and $\overline{D}$ the directivity term. The directivity term is different above and below a threshold frequency that depends on chord and local inflow velocity.

The model was verified against the results presented in Figure 4 of Amiet, 1975, and code-to-code compared against the results generated at DTU Wind Energy in Denmark with the code HAWC2 (Bertagnolio et al., 2017), and at the Technical University of Munich (TUM) with the code Cp-Max (Sucameli et al., 2018). Note that both DTU and TUM implement the formulation of the Amiet model described in Paterson and Amiet, 1976, with TUM also implementing the model from Amiet, 1975. Only the results from the former model are reported here for TUM because those from Amiet, 1975 overlap those from OpenFAST.

The inputs to the models used for the comparison are listed in Table 1, and the results of the comparison for two sets of chordwise and spanwise directivity angles are shown in Figure 1.

Table 1. Inputs to the Turbulent Inflow Noise Models Used in the Verification Studies. Inputs correspond to those of the Lowest Spectrum from Figure 4 in Amiet, 1975.

Input	Unit	Value
Air density ρ	kg m^{-3}	1.225
Speed of sound c	m s^{-1}	340.270
Turbulent length scale L_t	m	0.032
Span length d	m	0.533
Observer distance r_e	m	2.134
Incident turbulence intensity I_1	-	0.044
Incident wind speed U_1	m s^{-1}	30.965
Mach number M	-	0.091
Chord c	m	0.457

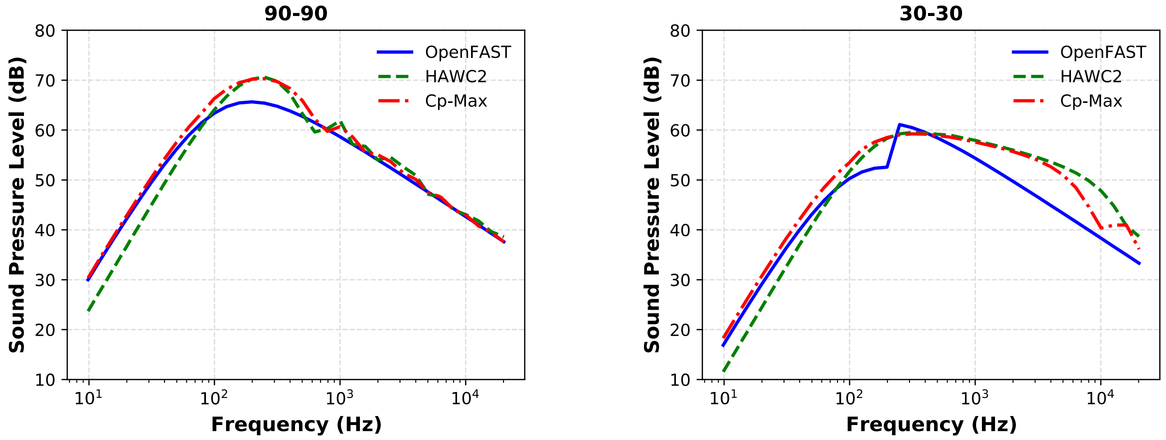

Figure 1. Results of the code-to-code verification of the turbulent inflow noise models applied at the airfoil level implemented in OpenFAST (NREL), HAWC2 (DTU), and Cp-Max (TUM). The left plot corresponds to an observer sitting on top of the airfoil LE, whereas the right plot corresponds to a case where chordwise and spanwise angles are both equal to 30 deg, see Figure 1 in Bortolotti et al., 2020 for a graphical representation of the angles.

At the airfoil level, the models are found to match fairly well. At chordwise and spanwise angles different than 90 degrees (i.e., for the observer not sitting on top of the airfoil LE), the model implemented in OpenFAST shows a discontinuity at the cut-off frequency because of the directivity term. Note that the directivity term at low frequency for the LE was originally missed in Bortolotti et al., 2020, which only reported directivity for the TE noise contribution. The documentation of OpenFAST v3.0.0 reports all formulas correctly (NREL, 2021).

2.2 Trailing edge noise

The second major source of aeroacoustics noise of wind turbines is noise that radiates from the TE of the blades. This noise source is usually referred to as turbulent boundary layer TE noise. OpenFAST implements two models to simulate this noise mechanism, namely the Brooks-Pope-Marcolini model (Brooks et al., 1989) and a more recent model implemented at the Dutch research institute TNO (Parchen, 1998). This work adopts the former model, which was code-to-code compared to the one available at TUM reporting minor discrepancies (Bortolotti et al., 2020).

Table 2. Key Characteristics of the GE 1.5-MW Wind Turbine.

Model	GE 1.5-MW SLE
Serial number	N000780-N/TB059-3
Configuration	Horizontal axis, upwind, three bladed
Control strategy	Pitch control, variable speed
Generator	Winergy, doubly fed induction, JFEC-500SS-06A
Gearbox	Winergy multistage planetary / helical model PEAB 4410.4, serial number NFR-W-111620
Blades	GE37c, fiberglass, S00028, S00029, S00030
Rated power (kW)	1,500
Rotor diameter (m)	77
Hub height (m)	80
Rated wind speed (m s^{-1})	14

3. Experimental Setup

An experimental campaign was conducted at the Flatirons Campus at NREL using an instrumented GE 1.5-MW wind turbine owned by the U.S. Department of Energy. The next two subsections briefly describe the equipment used and the measurement processing. Readers interested in the details of either topic should refer to an upcoming NREL technical report (Hamilton, 2021).

3.1 Equipment

The key characteristics of the GE 1.5-MW wind turbine are reported in Table 2, and a photo of the machine is shown on the left of Figure 2. This wind turbine model is representative of a large number of wind turbines operating in the United States, with more than 18,000 units installed.

The turbine installed at the Flatirons Campus has a permanent set of sensors measuring various quantities across the components. During this project, the area surrounding the wind turbine was further instrumented with 11 sound boards located as illustrated on the right of Figure 2.

Researchers chose the locations approximately symmetrical on either side of an axis aligned with the prevailing wind direction which, during the winter months, is equal to 285 degrees (Hamilton and Debnath, 2019). The international standards for wind turbine noise IEC 61400-11, for sound-level metering IEC 61672, and measurement microphones IEC 61094-4, were followed. Eight of the 11 microphones have a standard measurement range between 20 Hz and 11.2 kHz. The microphone marked as Mic 4C is one of these eight and is located at the IEC-prescribed location, downwind on the ground at a distance from tower base equal to the turbine height. The last three of the 11 microphones, located at the three data acquisition system (DAS) locations because of extra requirements in terms of power supply, are low-frequency microphones capable of measuring in the subaudible frequency range, as low as 1 Hz. The measurements of these microphones were not part of this study but will be used for future validations of the numerical framework to estimate the low frequency noise emissions of wind turbines.

Each microphone communicated with a DAS subsystem over coaxial connection. Signal degradation was mitigated in the instrumentation plan by limiting coaxial cable lengths to a maximum of 50 m (green lines in Figure 2). Communication from each DAS location to a central data storage server occurred over fiber-optic cables, which have less stringent constraints in terms of maximum distance.

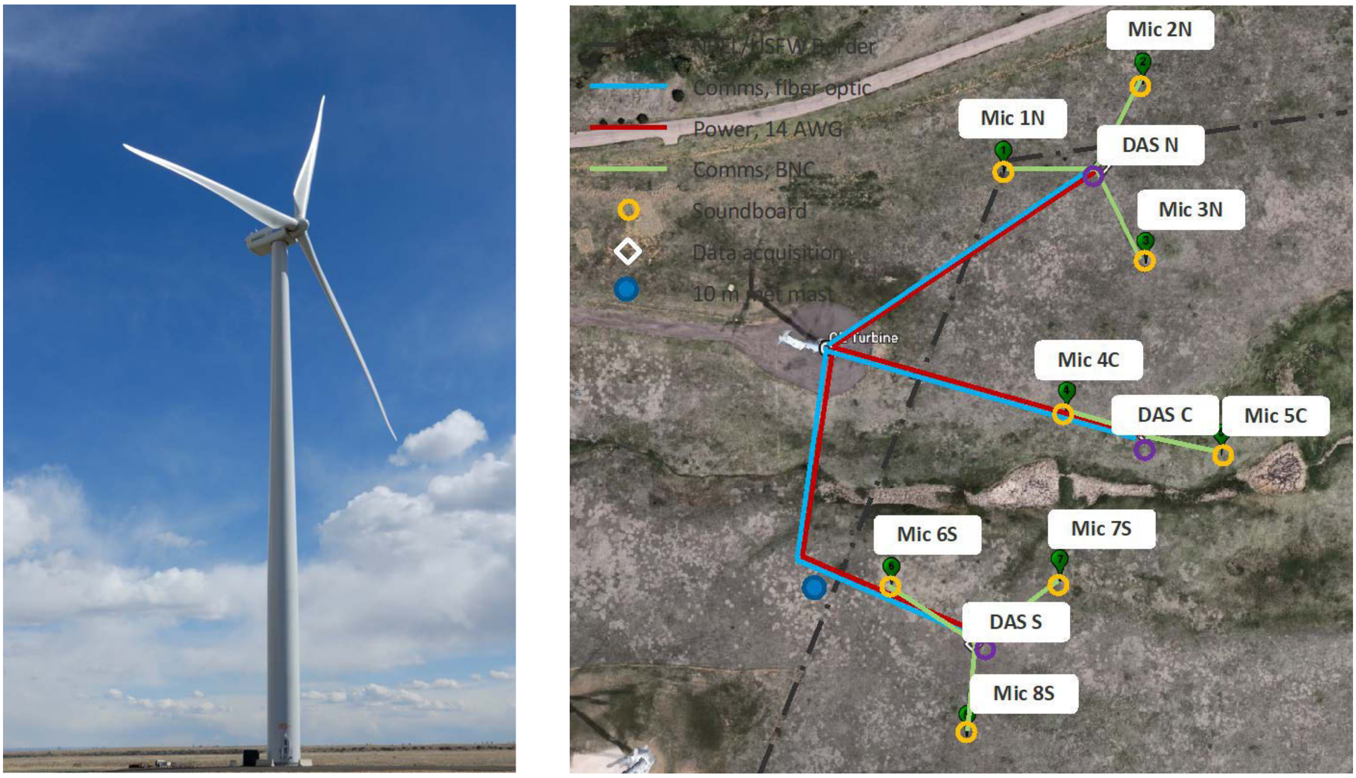

Figure 2. (Left) The GE 1.5-MW wind turbine located at the Flatirons Campus of NREL in Boulder, Colorado. (Right) Bird's-eye view of microphone locations and cabling. Mic 4C is at the IEC-prescribed location for a wind direction of 285 degrees.

3.2 Measurements and data processing

The measurement campaign took place between December 2020 and February 2021, with measurements obtained on eight different days. Because winter is the windy season at the Flatirons Campus of NREL, measurements could be obtained for a diverse set of wind speeds and atmospheric conditions for wind directions near 285 degrees. All microphones were calibrated at the beginning and at the end of each measurement period, and measurements were recorded during both day and night. Background noise was recorded by parking the wind turbine during a wide range of atmospheric conditions. Although not shown in Figure 2, reference wind speed measurements were obtained from a cup anemometer at 80-m height on a met tower located 153 m (2 rotor diameters) west of the wind turbine at a heading of 280 degrees. In addition, the turbulence intensity of the wind at different heights and at different average wind speeds was also reconstructed, and it is reported in Figure 3. Notably, all data streams were synchronized using Global Positioning System (GPS), which provided a way to not only synchronize the microphone data with the turbine and met tower data, but also to ensure that all recording windows for the microphones started at the same time and remained synchronized, greatly simplifying processing.

The rest of this section explains the data processing steps used to derive wind turbine SPLs binned by wind speed. First, for each microphone recording, the following steps are used to calculate unweighted and A-weighted SPLs in 10-second samples. Ten-second samples are used based on guidance in the IEC 61400-11 standard (International Electrotechnical Commission, 2020). For each 10-second sample, the unweighted 1/3-octave band SPL spectrum is calculated for center frequencies from 1 Hz to 20 kHz using the noiseLAB software (DELTA Acoustics and Vibration, 2014). The equivalent overall SPL is formed by energy summing the individual 1/3-octave bands (International Electrotechnical Commission, 2020). Similarly, the A-weighted 1/3-octave band SPL spectrum is calculated by applying the A-weighting transfer function to the unweighted 1/3-octave bands. The individual A-weighted 1/3-octave bands are then summed to determine the equivalent A-weighted SPL.

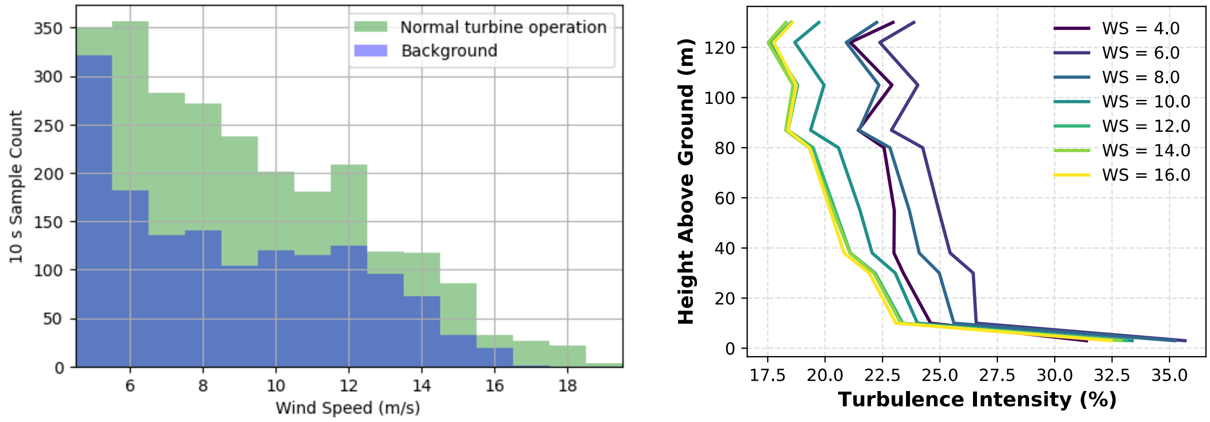

Figure 3. (Left) Number of valid 10-second SPL samples obtained for each 1 m s^{-1} wind speed bin for background and normal operation periods. (Right) Turbulence intensity versus height above ground at various average wind speeds at hub height.

Supervisory control and data acquisition (SCADA) data from the wind turbine and meteorological measurements from the met tower, sampled at a rate of 1 Hz, are processed into 10-second mean values and synchronized with the SPL samples. Together with the reference wind speed measurements at 80-m height from the met tower, the following two variables are used in the remainder of the data processing. Wind direction is estimated using the wind turbine's nacelle orientation, following guidance provided by the IEC 61400-11 standard (International Electrotechnical Commission, 2020). A turbine status signal indicating the operating state of the wind turbine is used to separate the data into background and normal operation categories.

After separating the synchronized noise, SCADA, and met tower data into background and normal operation periods, 10-second samples in which the nacelle position is more than 15 degrees from the intended wind direction of 285 degrees are removed, as recommended by the IEC 61400-11 standard. However, because of a lack of background measurement data, we do not apply any wind direction filtering to the background noise periods.

Lastly, noise data from the valid 10-second samples are binned by wind speed, using a bin width of 1 m s^{-1}. The number of 10-s samples for background and normal operation periods, binned by wind speed, are shown in Figure 3. Note that the IEC 61400-11 standard recommends a minimum of ten 10-s samples for background and normal operation periods within a wind speed bin. Based on this guidance, we analyze SPLs for wind speed bins up to 16 m s^{-1}.

Prior to using the noise measurements for model validation, the SPLs within a particular wind speed bin are averaged and the wind turbine noise is distinguished from background noise (e.g., wind-induced noise). For the SPL variable of interest, the data for both the background and normal operation periods are energy averaged using the following formula:

$$SPL_{\text{avg}} = 10 \log_{10} \left(\frac{1}{N} \sum_{i=1}^{N} 10^{\frac{SPL_i}{10}} \right), \tag{2}$$

where SPL_i represents the SPL for the *i*th 10-second sample in the wind speed bin and *N* indicates the number of samples in the bin. The average background SPL is then subtracted from the average SPL during normal operation, yielding the SPL attributed to wind turbine noise. Examples of the unweighted and A-weighted 1/3-octave band SPL spectra for normal operation and background periods, along with the spectra representing wind turbine noise, for the 10 m s^{-1} wind speed bin are provided in Figure 4. Note that for frequencies below 315 Hz in this wind speed bin, the background noise is greater than the total noise when the turbine is operating.

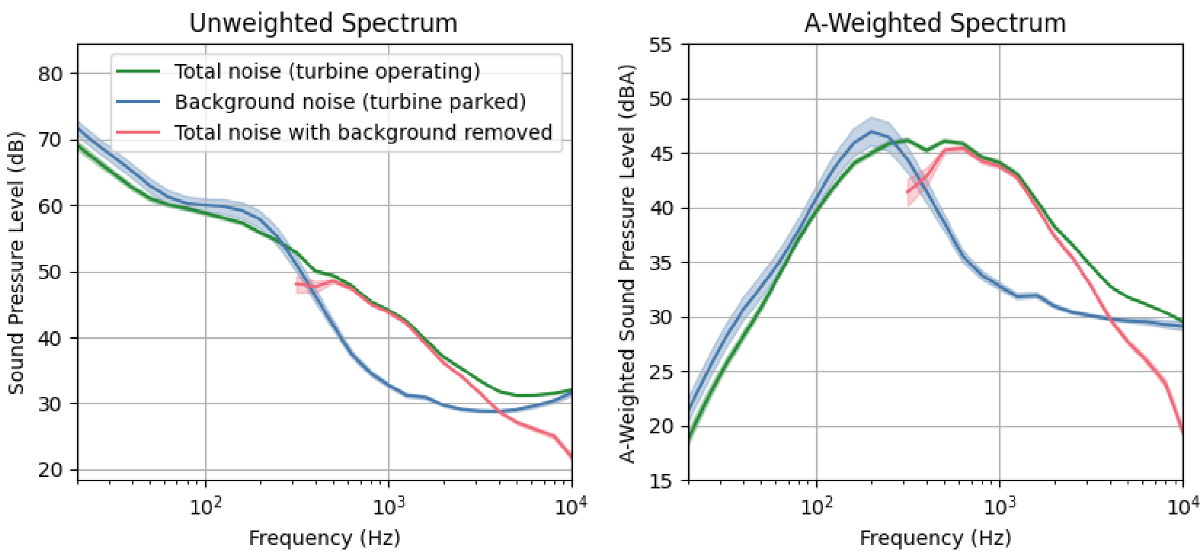

Figure 4. Unweighted (left) and A-weighted (right) 1/3-octave band SPL spectra for the 10 m s^{-1} wind speed bin. Energy averaged spectra for normal operation and background periods are shown together with the spectra for normal operation with background noise removed (i.e., the spectra attributed to wind turbine noise). The shaded regions indicate the standard error associated with the energy averaged SPL estimates.

Therefore, the SPL attributed to wind turbine noise cannot be calculated for these frequencies. Ideally, background noise should not exceed the combined background and wind turbine noise. But in this data set, the background noise measurements were likely obtained in different atmospheric conditions (e.g., with higher turbulence intensity) than the normal operation periods, leading to higher low-frequency wind-induced noise levels.

4. Validation

This section presents the comparison between the numerical predictions of OpenFAST and the field measurements of the noise emissions of the GE 1.5-MW turbine. The overall SPLs between 10 Hz and 20 kHz are compared at various wind speeds for the eight standard microphones described in Section 3.1. The OpenFAST simulations are run with the same rotor speed and pitch angle of the real turbine. The simulations are run at steady wind speed, and time-invariant turbulence intensities are assumed for the LE noise model. The turbulence intensity is assumed to follow the lines shown in Figure 3. The numerical simulations also assume a turbulent length scale of 42 m, which is the value prescribed by the IEC 61400-11 standard.

Figure 5 shows the SPL spectrum predicted by OpenFAST in comparison with the experimental results for average wind speeds at hub heights of 6 m s^{-1}, 8 m s^{-1}, 10 m s^{-1}, and 12 m s^{-1} for the microphone 4C, which is located at the IEC-prescribed location. Overall, fairly good agreement between OpenFAST and experimental results is reported at 8 m s^{-1} and 10 m s^{-1}, whereas OpenFAST underpredicts SPL at 6 m s^{-1} and overpredicts at 12 m s^{-1}. At frequencies less than 0.2 kHz, experimental data is unavailable because the background noise matches the intensity of turbine noise. When frequencies move beyond 0.2 kHz to 0.3 kHz, the TE noise starts dominating the spectrum and both numerical and experimental lines show a bump. Notably, at 10 m s^{-1} and 12 m s^{-1}, and at frequencies higher than 2 kHz, the OpenFAST predictions start to deviate from experimental data. The discrepancy may originate from the turbulent boundary layer TE noise component of the Brooks-Pope-Marcolini model. Another source of error could be the high background noise, which above 4 kHz is higher than the turbine noise with background removed, see Figure 4.

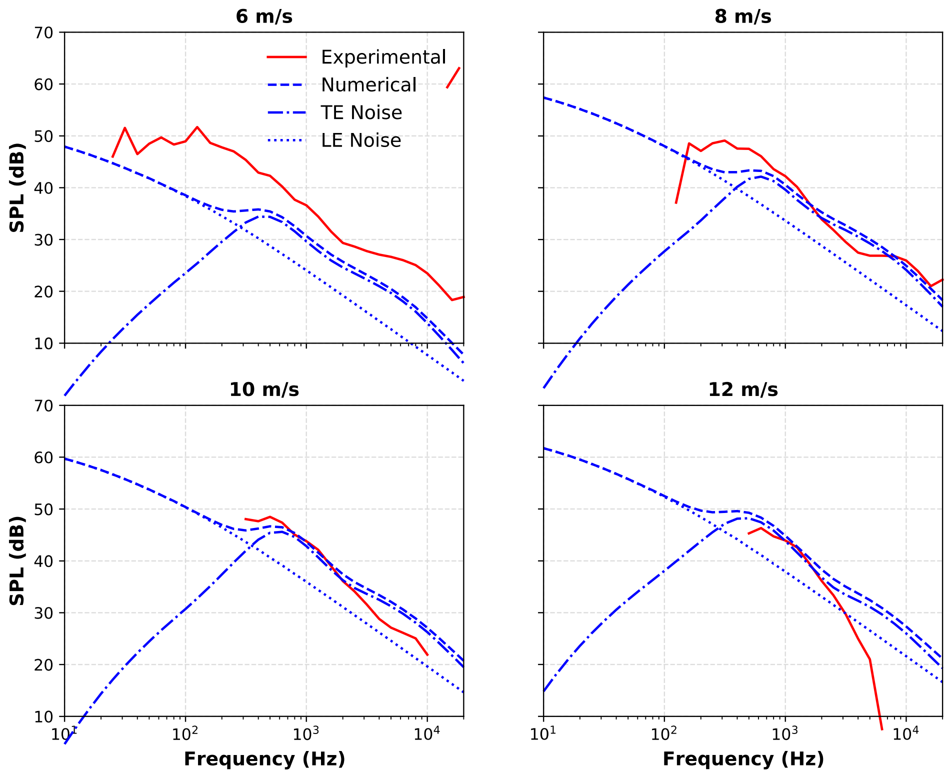

Figure 5. Numerical and experimental frequency spectra of the sound pressure levels (SPLs) at four wind speeds at IEC-prescribed location Mic 4C. The numerical predictions are the sum of LE and TE noise.

Future work will investigate if the TNO model, combined with accurate descriptions of the boundary layer characteristics along blade span, can reduce the gap.

Figure 6 compares the measured and numerical overall SPLs at various wind speeds at all eight microphone locations. The validation shows a somewhat surprising different slope with respect to wind speed. OpenFAST predicts a more marked dependency of the overall A-weighted SPL (OASPL) to wind speed primarily caused by variations in rotor speed, whereas the experimental recordings show a milder dependency. The differences are highest at 6 m s^{-1} and are between 5 dB(A) and 7 dB(A), depending on the microphone. Mic 2N also shows a discrepancy of 10 dB(A) at 14 m s^{-1}, but the experimental recording that decreases with wind speed suggests that the experimental data point may be flawed. Finally, Mic 6S reports the poorest comparison with the experimental line above the numerical one by 7 dB(A) at 6 m s^{-1} and by 4 dB(A) at 10 m s^{-1}. The fact that Mic 6S is located near a hill might be making the comparison more challenging than for the other microphones.

5. Conclusions and Ongoing Activities

This work presents the latest update of the aeroacoustics model in the wind turbine aeroservoelastic solver, OpenFAST, and its validation against measurements recorded on a GE 1.5-MW machine installed at the Flatirons Campus of NREL. The validation returns differences up to 3 dB(A) between numerical and experimental lines in the range of 8 m s^{-1} to 12 m s^{-1} of wind speed at hub height, but errors up to 7 dB(A) outside this range. The discrepancies are generated by the different slope of the overall SPLs in respect to wind speed, with OpenFAST predicting a steeper curve, whereas the experimental recordings are found less sensitive to wind speed.

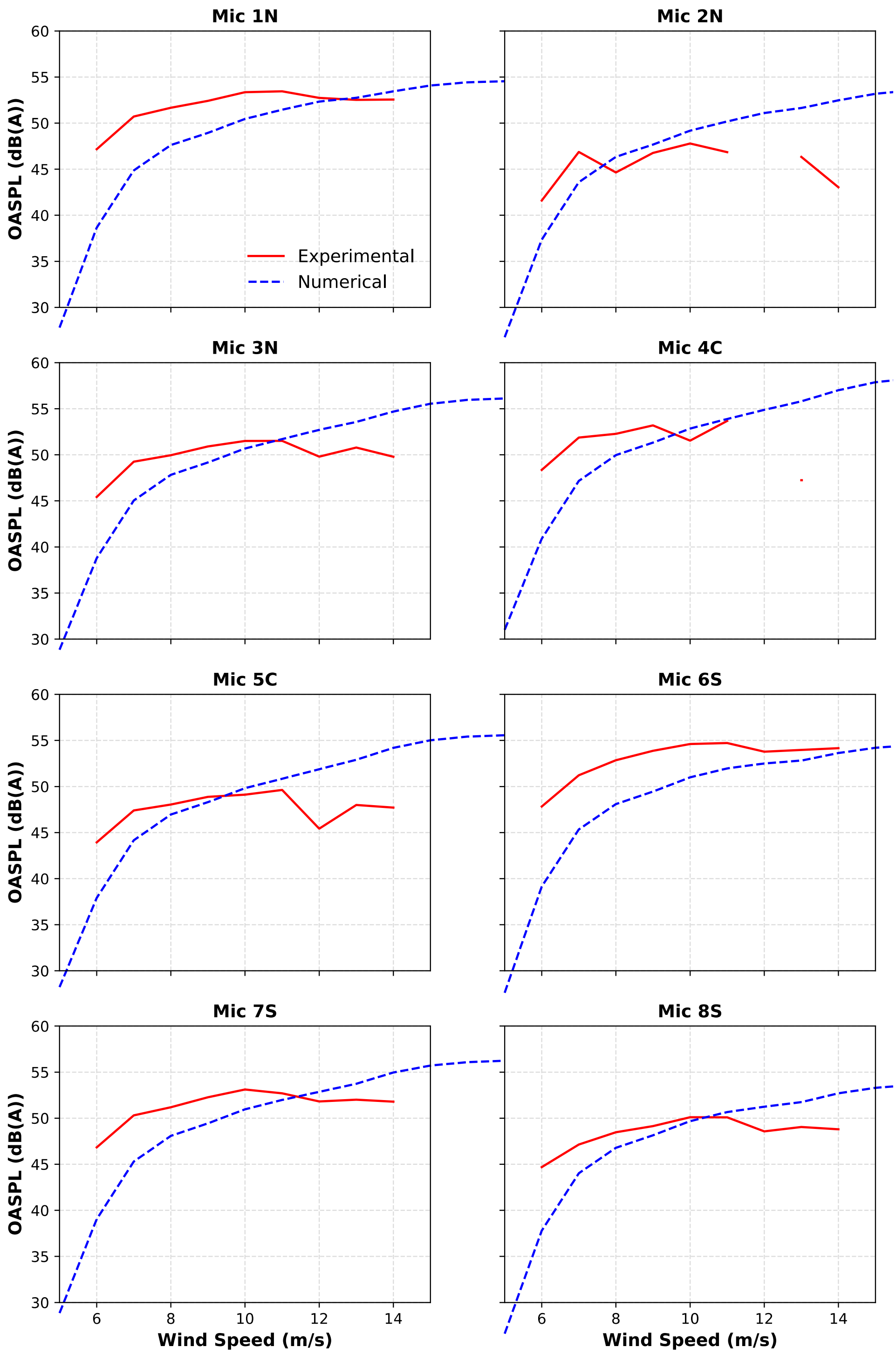

Figure 6. Numerical and experimental overall A-weighted sound pressure levels (OASPL) at the eight microphone locations at varying wind speeds.

Several activities are ongoing. The verification step presented in Section 2 was restricted to the airfoil level and only to three numerical frameworks. Studies within the IEA Wind Task 39 on Quiet Wind Turbine Technology are comparing the outputs of multiple codes at the turbine level. The comparison is based on the NM80 wind turbine located at the Danish research center Risø. A dedicated technical report is being prepared. In addition, the validation process should include the other noise models implemented in OpenFAST, such as the LE model described in Moriarty et al., 2005, and the TE noise model described in Parchen, 1998. Finally, more work is required on processing of low-frequency noise measurements, first focusing on distinguishing the turbine noise from the background and later validating the models available at DTU and TUM, among others.

Acknowledgments

The authors would like to acknowledge the precious work of the field technicians of NREL. This work was authored by the National Renewable Energy Laboratory, operated by Alliance for Sustainable Energy, LLC, for the U.S. Department of Energy (DOE) under Contract No. DE-AC36-08GO28308. Funding provided by the U.S. Department of Energy Office of Energy Efficiency and Renewable Energy Wind Energy Technologies Office. The views expressed in the article do not necessarily represent the views of the DOE or the U.S. Government. The U.S. Government retains and the publisher, by accepting the article for publication, acknowledges that the U.S. Government retains a nonexclusive, paid-up, irrevocable, worldwide license to publish or reproduce the published form of this work, or allow others to do so, for U.S. Government purposes.

References

Amiet RK (1975) *Acoustic Radiation from an Airfoil in a Turbulent Stream* Journal of Sound and Vibration 41(4), 407-420 doi: 10.1016/S0022-460X(75)80105-2

Bertagnolio F, Madsen HAa, and Fischer A (2017) *A Combined Aeroelastic-Aeroacoustic Model for Wind Turbine Noise: Verification and Analysis of Field Measurements* 20(8), 1331-1348 doi: 10.1002/we.2096

Bortolotti P, Branlard E, Platt A, Moriarty PJ, Sucameli C, and Bottasso CL (2020) *Aeroacoustics Noise Model of OpenFAST* NREL/TP-5000-75731

Brooks TF, Pope DS, and Marcolini MA (1989) *Airfoil self-noise and prediction* NASA Reference Publication 1218

DELTA Acoustics and Vibration (2014) "noiseLAB User's Guide for Version 4.0". https://noiselabdk.files.wordpress.com/2011/10/noiselab-4-0-users-guide.pdf

Hamilton N, and Debnath MC (2019) *National Wind Technology Center-Characterization of Atmospheric Conditions* NREL/TP-5000-72091

Hamilton N, Bortolotti P, Simley E, Guo Y, and Roadman J (2021) *Aeroacoustic Assessment of Wind Plant Controls*. NREL Technical Report. In Preparation

International Electrotechnical Commission (2020) "International Electrotechnical Commission (IEC) standard, Wind Turbines Part 11: Acoustic Noise Measurement Techniques". IEC 61400-11, Edition3.1

Moriarty PJ (2005) *NAFNoise User's Guide* https://www.nrel.gov/wind/nwtc/assets/pdfs/nafnoise.pdf

Moriarty PJ, and Migliore P (2003) *Semi-Empirical Aeroacoustic Noise Prediction Code for Wind Turbines* NREL/TP-500-34478

Moriarty PJ, Guidati G, and Migliore P (2005) *Prediction of Turbulent Inflow and Trailing-Edge Noise for Wind Turbines* 11th AIAA/CEAS Aeroacoustics Conference

NREL (2021) *OpenFAST Documentation - Read the Docs v3.0.0*

Parchen RR (1998) *Progress Report DRAW: A Prediction Scheme for Trailing Edge Noise Based on Detailed Boundary Layer Characteristics* TNO Institute of Applied Physics

Paterson RW, and Amiet RK (1976) *Acoustic radiation and surface pressure characteristics of an airfoil due to incident turbulence* NASA Contractor Report 2733

Sucameli CR, Bortolotti P, Croce A, and CL Bottasso (2018) *Comparison of some wind turbine noise emission models coupled to BEM aerodynamics* J. Phys.: Conf. Ser. 1037 022038